THE JOURNAL OF BIOLOGICAL CHEMISTRY VOL. 285, NO. 43, pp. 33475–33484, October 22, 2010

A Specific Docking Site for DNA Polymerase α-Primase on the SV40 Helicase Is Required for Viral Primosome Activity, but Helicase Activity Is Dispensable*

Received for publication, June 18, 2010, and in revised form, July 31, 2010 Published, JBC Papers in Press, August 3, 2010, DOI 10.1074/jbc.M110.156240

Hao Huang, Kun Zhao, Diana R. Arnett, and Ellen Fanning[1]

From the Department of Biological Sciences, Vanderbilt University, Nashville, Tennessee 37235-1634

Replication of simian virus 40 (SV40) DNA, a model for eukaryotic chromosomal replication, can be reconstituted *in vitro* using the viral helicase (large tumor antigen, or Tag) and purified human proteins. Tag interacts physically with two cellular proteins, replication protein A and DNA polymerase α-primase (pol-prim), constituting the viral primosome. Like the well characterized primosomes of phages T7 and T4, this trio of proteins coordinates parental DNA unwinding with primer synthesis to initiate the leading strand at the viral origin and each Okazaki fragment on the lagging strand template. We recently determined the structure of a previously unrecognized pol-prim domain (p68N) that docks on Tag, identified the p68N surface that contacts Tag, and demonstrated its vital role in primosome function. Here, we identify the p68N-docking site on Tag by using structure-guided mutagenesis of the Tag helicase surface. A charge reverse substitution in Tag disrupted both p68N-binding and primosome activity but did not affect docking with other pol-prim subunits. Unexpectedly, the substitution also disrupted Tag ATPase and helicase activity, suggesting a potential link between p68N docking and ATPase activity. To assess this possibility, we examined the primosome activity of Tag with a single residue substitution in the Walker B motif. Although this substitution abolished ATPase and helicase activity as expected, it did not reduce pol-prim docking on Tag or primosome activity on single-stranded DNA, indicating that Tag ATPase is dispensable for primosome activity *in vitro*.

De novo DNA replication begins with RNA primer synthesis on single-stranded template DNA, followed by primer extension by a processive DNA polymerase. In prokaryotic replication, the activity of the primase is coordinated with unwinding of duplex DNA by a hexameric replicative helicase and a single-stranded DNA (ssDNA)[2]-binding protein, largely through dynamic physical interactions among the three proteins, which constitute a primosome (1–4). In eukaryotes, the DNA polymerase α-primase (pol-prim) complex catalyzes both RNA primer synthesis and extension, yielding RNA-DNA primers of 30–35 nucleotides (5, 6). Unlike the single subunit prokaryotic primases, pol-prim is a stable heterotetramer composed of the primase heterodimer p48/p58, the catalytic DNA polymerase subunit p180, and a regulatory subunit (B or p68) (7). The eukaryotic replicative helicase complex, Cdc45/Mcm2–7/GINS, and the ssDNA-binding protein, replication protein A (RPA), appear to coordinate primer synthesis by pol-prim with parental DNA unwinding, as in prokaryotes (8–12). However, the nature of the eukaryotic primosome and its operation during chromosome replication, telomere maintenance, and checkpoint signaling at stalled replication forks remain elusive.

Because pol-prim is essential for replication of simian virus 40 (SV40) DNA, we utilize this model system here to investigate the functional architecture of a eukaryotic primosome. SV40 DNA replication can be reconstituted in cell-free reactions with purified recombinant human proteins and the viral large T antigen (Tag) (13). Tag serves as the replicative helicase and orchestrates the assembly of the viral replisome. Tag monomers first assemble cooperatively into a preinitiation complex on the viral origin of DNA replication, forming two hexamers oriented head-to-head, akin to the Mcm2–7 (minichromosome maintenance 2–7) hexamer assemblies recently visualized on yeast origins (14–16). To initiate replication, the preinitiation complex rearranges into a bidirectional minireplication factory (14, 17–20). As Tag unwinds parental DNA, it interacts physically with two different surfaces of RPA and actively loads it onto the emerging template via a transient ternary complex with RPA/ssDNA, thereby coupling DNA unwinding with RPA deposition (21–24). Tag also interacts physically with at least three subunits of pol-prim (25–31). These interactions led to a model of SV40 primosome activity in which Tag contacts with RPA/ssDNA remodel RPA into a weaker ssDNA-binding mode, transiently affording local access to the template (Fig. 1*A*). Tag can then load its associated pol-prim onto RNA-ssDNA in a molecular handoff reaction that enables primer synthesis (22, 32–35). Thus, physical interactions among pol-prim, Tag, and RPA are proposed to contribute to primosome activity in the SV40 replisome.

To gain greater insight into the operation of the SV40 primosome, we recently identified a previously unrecognized domain of the pol-prim p68 subunit (p68N) that docks on Tag, determined its solution structure, and identified the surface of p68N that docks on Tag (36). Structure-guided mutagenesis of p68N

* This work was supported, in whole or in part, by National Institutes of Health Grants GM52948 (to E. F.) and P30 CA068485 (to the Vanderbilt-Ingram Cancer Center). This work was also supported by Vanderbilt University and the Alexander von Humboldt Foundation.

[1] To whom correspondence should be addressed. Tel.: 615-343-5677; Fax: 615-343-6707; E-mail: Ellen.fanning@vanderbilt.edu.

[2] The abbreviations used are: ssDNA, single-stranded DNA; AAA+, ATPases associated with various cellular activities; OBD, origin DNA-binding domain; Pab101, polyomavirus monoclonal antibody 101; pol-prim, DNA polymerase α-primase; RPA, replication protein A; Tag, large tumor antigen; P4, patch 4 mutant.

was used to confirm its Tag-docking surface. Substitutions in this surface that specifically reduced its affinity for Tag were then introduced into the intact pol-prim complex and shown to diminish SV40 primosome activity. The results demonstrated that p68-Tag docking is vital for primosome activity, even in the presence of p180 and primase docking on Tag, supporting a working model in which this network of contacts may position pol-prim to access the exposed template. This model implies the existence of a corresponding docking site for p68N on the surface of Tag. Localization of pol-prim-docking sites on Tag would provide new insight into the architecture of the primosome and coordination of its activity with that of the helicase.

Here we report the identification of the predicted p68N-docking site on the C-terminal face of the Tag helicase domain, show that a Tag variant unable to bind to p68 retains binding to p180 and primase, and demonstrate the importance of p68-Tag interaction in primosome activity. In addition, we report that the ATPase/translocase activity (and hence helicase activity) of Tag is dispensable for primosome activity *in vitro*. Potential implications of our data for the overall architecture of the SV40 primosome and the coordination of priming with parental DNA unwinding are discussed.

EXPERIMENTAL PROCEDURES

Yeast Two-hybrid Assay—Coding sequences of Tag fragments were amplified by PCR and ligated into the EcoRI/BamHI sites of pGADT7 vector containing a *Trp* selection marker (Clontech). Coding sequences of p68 fragments were amplified by PCR and ligated into the NdeI/BamHI sites of pGBKT7 vector containing a *Leu* selection marker. These plasmids were co-transformed into yeast strain AH109, which contains three reporter genes, *His3, Ade2*, and *LacZ*. The cells were allowed to grow 4 days on −Leu −Trp plates. Positive colonies were picked and streaked on a −Leu −Trp plate and on a −Leu −Trp −His −Ade plate. Plates were photographed after growth for another 4 days.

Protein Expression and Purification—Wild type (WT) and mutant SV40 Tag and topoisomerase I were expressed in insect cells using recombinant baculoviruses and purified as described (22). Pol-prim was expressed in Hi-5 insect cells infected with four recombinant baculoviruses and purified by immunoaffinity chromatography as described previously (31). Bacterially expressed His-p68 (31) and p48/p58 human primase (37, 38) were prepared as described. Recombinant human RPA was expressed in *Escherichia coli* and purified as described (39).

The DNA encoding pol-prim p68 1–107 was amplified by PCR, verified by DNA sequencing, and ligated into the BamHI/NotI sites of a modified pET-32a plasmid (36). Thioredoxin-His-tagged pol-prim p68 1–107 and p180 1–323 fragments were purified using nickel-nitrilotriacetic acid affinity chromatography. Coding sequences of Tag fragments 131–259, 251–627, 303–627, and 357–627 were PCR-amplified, cloned into the BamHI/EcoRI sites of the pGEX-2T expression vector (GE Healthcare), and verified by DNA sequencing. Glutathione *S*-transferase (GST) fusion proteins were expressed in *E. coli* BL21 (DE3) cells and purified using glutathione-agarose affinity chromatography.

Tag Pull-down Assays—Purified Tag was bound to monoclonal antibody Pab101-coupled Sepharose beads, or GST-tagged Tag fragments (10 μg) were bound to glutathione-agarose beads. The protein-bound beads were then incubated with His-p68, His-p68 1–107, His-p180 1–323, or primase (as stated in the figure legends) in binding buffer (30 mM HEPES-KOH, pH 7.8, 10 mM KCl, 7 mM $MgCl_2$) containing 2% nonfat dry milk for 1 h at 4 °C with end-over-end rotation. The beads were washed once with binding buffer, three times with wash buffer (30 mM HEPES-KOH, pH 7.8, 25 mM KCl, 7 mM $MgCl_2$, 0.25% inositol, 0.01% Nonidet P-40), and once with binding buffer. For Pab101 pull-downs, binding and wash buffers were supplemented with 10 μM $ZnCl_2$. The beads were resuspended in 30 μl of 2× SDS-PAGE loading buffer and heated at 100 °C for 5 min. Samples were analyzed by SDS-PAGE and visualized by immunoblotting with monoclonal Pab101 for Tag (40), rabbit anti-GST (Invitrogen) for Tag fusion proteins, anti-His (Abcam 9801 or Genscript A00186) for His-tagged proteins, rat PRI-8G10 for p48 (30), and chemiluminescence (PerkinElmer Life Sciences).

Tag Helicase Assay—To prepare the helicase substrate, a 33-nucleotide oligonucleotide (5′- TCGACTCTAGAGGATC-CCCGGGTACCGAGCTCG) was labeled at the 5′-end with [γ-^{32}P]ATP by T4 polynucleotide kinase (New England Biolabs) and annealed to M13mp18 ssDNA (U.S. Biochemical Corp.). Approximately 10 fmol of substrate was incubated with WT or mutant Tag (2, 4, or 6 pmol) for 45 min at 37 °C in a 15-μl reaction consisting of 20 mM Tris (pH 7.5), 10 mM $MgCl_2$, 4 mM ATP, 0.1 μg/μl bovine serum albumin, and 1 mM DTT. Reactions were terminated by the addition of SDS to 0.25% and EDTA to 50 mM, separated by electrophoresis in 12% native acrylamide gels in 0.5× Tris borate EDTA buffer, and visualized using a PhosphorImager (Amersham Biosciences).

Tag ATPase Assay—WT or mutant Tag (0.5, 1.0, or 1.5 μg) was added to a reaction mixture (20 μl) containing 50 pmol of ATP and 1 μCi of [α-^{32}P]ATP (3000 Ci/mmol; PerkinElmer Life Sciences) in 50 mM Tris-HCl (pH 8), 10 mM NaCl, 7 mM $MgCl_2$, 0.05% Nonidet P-40, 1 mM DTT. After 10 min at 37 °C, 1 μl of 1% SDS, 40 mM EDTA was added to terminate the reaction. 1 μl of the reaction mixture was spotted onto polyethyleneimine-cellulose F thin layer chromatography plates (EMD Chemicals), and the plates were developed in 1 M formic acid, 0.5 M LiCl. After the plates dried, released phosphate and remaining ATP were visualized by autoradiography.

Initiation of SV40 DNA Replication—Monopolymerase assays (41) were carried out as described previously (22). Briefly, reaction mixtures (20 μl) contained 250 ng of supercoiled pUC-HS plasmid DNA, 200 ng of RPA, 300 ng of topoisomerase I, 600 ng of Tag and 50–200 ng of recombinant pol-prim in initiation buffer (30 mM HEPES-KOH, pH 7.9, 7 mM magnesium acetate, 10 μM $ZnCl_2$, 1 mM DTT, 4 mM ATP, 0.2 mM each GTP, UTP, and CTP, 0.1 mM each dGTP, dATP, and dTTP, 0.02 mM dCTP, 40 mM creatine phosphate, 40 μg/ml creatine kinase) supplemented with 3 μCi of [α-^{32}P]dCTP (3000 Ci/mmol). Reaction mixtures were assembled on ice, incubated at 37 °C for 90 min, and then digested with 0.1 mg/ml proteinase K in the presence of 1% SDS and 1 mM EDTA at 37 °C for 30 min. Radiolabeled reaction products were purified on G-50

Sephadex columns and precipitated with 2% $NaClO_4$ in acetone. The products were washed, dried, resuspended in alkaline loading buffer (60 mM NaOH, 2 mM EDTA (pH 8.0), 20% [w/v] Ficoll, 0.1% (w/v) bromphenol blue, 0.1% (w/v) xylene cyanol), and electrophoresed on 1.5% agarose gels in running buffer (30 mM NaOH, 1 mM EDTA). The gels were fixed in 10% TCA and dried. The reaction products were visualized by autoradiography and quantified by densitometry or phosphorimaging.

Primer Synthesis and Elongation in the Presence of RPA—Reaction mixtures (20 μl) containing 100 ng of single-stranded M13 DNA were preincubated with 1000 ng of RPA in initiation buffer (see above) at 4 °C for 20 min. The reactions then were supplemented with 3 μCi of [α-^{32}P]dCTP, 200–600 ng of Tag, and 600 ng of pol-prim as indicated in the figure legends, incubated at 37 °C for 45 min, and then digested with 0.1 mg/ml proteinase K in the presence of 1% SDS and 1 mM EDTA at 37 °C for 30 min. Radiolabeled reaction products were then processed and analyzed as described above for the monopolymerase assay.

RESULTS

The AAA+/D3 Subdomains of Tag Interact with the p68 Subunit of pol-prim—Tag is a modular protein composed of three major domains linked through flexible peptides and a C-terminal region of unknown structure (Fig. 1*B*). Using yeast two-hybrid assays, we recently demonstrated that the N-terminal domain of p68 (residues 1–78 and 1–107) interacts physically with the helicase domain of Tag (36). To confirm the Tag-p68 mapping data, bacterially expressed, purified GST-Tag constructs were tested for their ability to bind to purified p68 1–107 in pull-down assays. No p68 interaction was detected with the origin DNA-binding domain of Tag (residues 131–259) (Fig. 1*C*, *lanes 2* and *3*), but all three GST-Tag fragments containing the AAA+/D3 region (residues 357–627) pulled down the p68 fragment in a concentration-dependent manner (*lanes 4–9*). The results demonstrate that the AAA+/D3 subdomains of Tag bind specifically and directly to the N terminus of p68.

Mapping the p68-interacting Surface of the Tag Helicase Domain—Crystal structures of the hexameric Tag helicase domain reveal a "double-donut" structure consisting of the six zinc subdomains (residues 251–356) in a smaller ring and the six AAA+ (ATPases associated with a variety of cellular activities) subdomains and the surrounding helices of the D3 subdomains (residues 357–627) in a larger ring (42–44) (Fig. 2*A*). These structures provide a foundation for mapping the binding sites of pol-prim subunits on the surface of Tag.

Based on the hydrophobic and acidic character of the Tag-binding surface of p68N (36), we reasoned that the p68N-binding surface of Tag would be likely to display some positive charge. To search for such a surface on the helicase domain, we utilized a recently generated panel of amino acid substitutions in conserved, surface-exposed residues, which was designed using structural models of the hexameric helicase domain (42, 43, 45). Use of the hexamer structure to identify surface residues for mutagenesis should minimize substitutions that would cause gross structural perturbations of the protein or interfere with its oligomerization. Clusters of charged surface residues were grouped to generate a panel of five "patch mutants," each

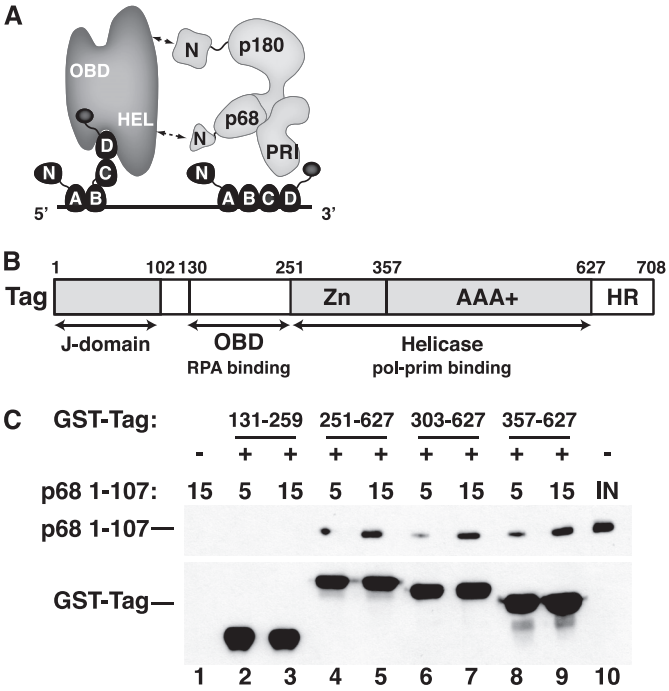

FIGURE 1. **Tag 357–627 is sufficient to bind to pol-prim p68 1–107.** *A*, a molecular handoff model for SV40 primosome activity on RPA-coated ssDNA. The four ssDNA-binding domains (*A–D*) of RPA (*dark gray*) occlude up to 30 nucleotides of ssDNA (*straight line*). Flexible linkers (*wavy lines*) join the N-terminal domain of RPA70 and the C-terminal domain of RPA32 to the RPA/ssDNA. Tag contacts with RPA32C and RPA70AB remodel it into a more compact, lower affinity ssDNA-binding mode and stabilize it as a ternary complex (22, 23, 35), transiently exposing the template ssDNA. pol-prim (*light gray*) contacts the Tag helicase domains (*HEL*) through p68N (36), the N terminus of p180 DNA polymerase, and unknown surfaces of primase p58/p48 (*PRI*) (27, 29, 30). The ensemble of these interactions is proposed to position primase on the exposed template to synthesize an RNA primer (not shown). *B*, domain architecture of SV40 Tag. The DnaJ chaperone domain (72), SV40 OBD (73), and helicase domain (42, 43) are depicted. The structure of the host-range (*HR*) domain is not known (74). *C*, GST-tagged Tag fragments 131–259 (*lanes 2* and *3*), 251–627 (*lanes 4* and *5*), 303–627 (*lanes 6* and *7*), or 357–627 (*lanes 8* and *9*) adsorbed to glutathione beads were incubated with increasing amounts of His-tagged p68 1–107 as indicated. Proteins bound to the beads were separated by SDS-PAGE and visualized by Western blotting with anti-His antibody (*top*) or anti-GST antibody (*bottom*). Glutathione beads lacking GST-Tag protein (*lane 1*) are shown as negative control. *Lane 10* shows 200 ng of input p68 1–107.

containing four charge reverse substitutions (Fig. 2*A*) (45). Four patch mutants were screened in yeast two-hybrid assays for interaction with p68 1–107. The initial screen demonstrated that p68 1–107 interacted with WT and patch mutants 1–3 but failed to interact with the patch 4 cluster containing K425E, R483E, K535E, and K543E substitutions (Fig. 2*B*, *sector 5*). A second round of screening was conducted using a series of Tag constructs, each with one of the substitutions from patch 4. In this screen, the p68 fragment interacted well with WT Tag 357–627 and all of the single charge reverse proteins except K425E (Fig. 2*C*, *sector 6*).

To strengthen the two-hybrid results, pull-down experiments were conducted with purified GST-Tag 357–627 constructs and p68 1–107. The WT GST-Tag construct pulled down the p68 fragment, but the patch 4 mutant (P4) and the K425E mutant constructs displayed little or no interaction with the p68 N terminus (Fig. 2*D*, compare *lanes 2* and *3* with *lanes 4–7*). These results indicate that a direct interaction between Tag and p68 1–107 is disrupted by the K425E substi-

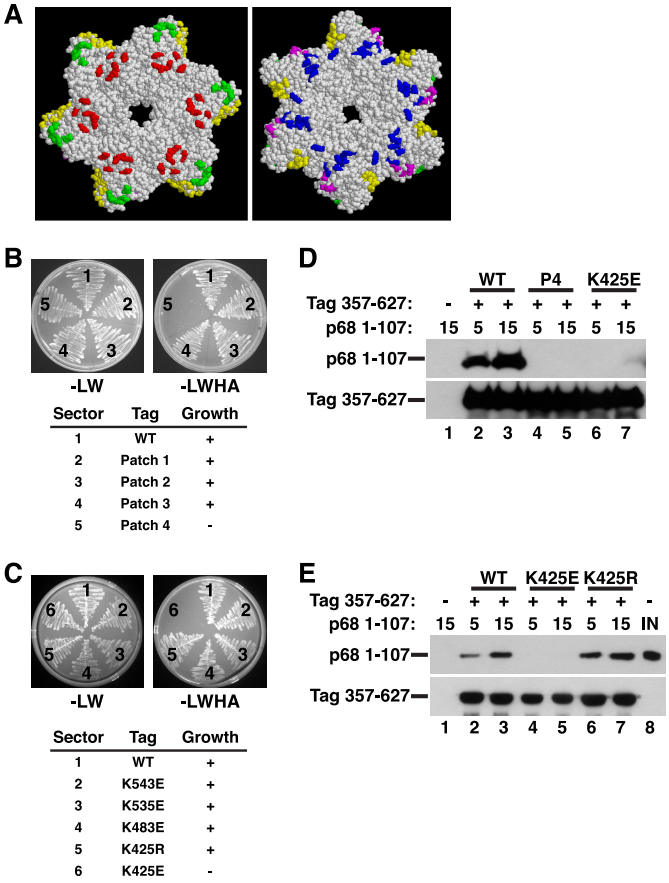

FIGURE 2. **Structure-guided mutagenesis of Tag surface residues to map the p68N-docking site.** *A*, diagram of conserved patches of charged surface residues of the Tag hexamer (residues 266–627) (45) (reprinted with permission). In the *left view*, the six zinc subdomains face the *reader*; the *right view* is rotated 180° so that the AAA+ subdomains face the *reader*. *Green*, patch 1; *yellow*, patch 2; *red*, patch 3; *blue*, patch 4; *magenta*, patch 5. Patch mutants (*B*) and single residue substitutions of pGADT7-fused Tag (*C*) were screened in yeast two-hybrid assays for interaction with pGBKT7-fused p68 1–107. The *numbered sectors* are identified in the *tables below*. *Left panel*, control plate -Leu -Trp; *right panel*, selective plate -Leu -Trp -His -Ade. *D*, glutathione beads alone (*lane 1*) or adsorbed to WT (*lanes 2* and *3*), patch 4 (*P4*) mutant (*lanes 4* and *5*), or K425E GST-Tag 357–627 (*lanes 6* and *7*) were incubated with 5 or 15 μg of His-tagged p68 1–107 as indicated. Bound proteins were analyzed by Western blotting with anti-His (*top*) or anti-GST antibody (*bottom*). *E*, glutathione beads alone (*lane 1*) or adsorbed to GST-Tag 357–627 WT (*lanes 2* and *3*), K425E (*lanes 3* and *4*), or K425R (*lanes 6* and *7*) were incubated with 5 or 15 μg of p68 1–107 as indicated. Bound proteins were analyzed by Western blotting with anti-His (*top*) or anti-GST antibody (*bottom*). *Lane 8* shows 200 ng of input p68 1–107.

tution in Tag. Pull-down experiments also showed that K425E, but not K425R, substantially reduced Tag 357–627 binding to p68 1–107 (Fig. 2*E*, compare *lanes 4* and *5* with *lanes 6* and *7*), confirming that the charge swap was responsible for the weakened interaction.

Mutation of the p68-interacting Surface of Full-length Tag Does Not Significantly Reduce Binding to p180 or Primase but Nearly Abolishes Primosome Activity—The mapping results in Figs. 1 and 2 suggest that the K425E substitution compromises Tag interaction with the p68 subunit of pol-prim. Together with evidence that p68 docking on Tag is vital for primosome activity (36), these findings predict that Tag K425E should display defective primosome activity. In order to test this prediction, we first generated the full-length recombinant K425E protein and characterized it. The purified mutant Tag was stable and obtained in yields comparable with that of WT Tag (Fig. 3*A*), suggesting that K425E Tag is folded reasonably well.

First, to test the possibility that the K425E substitution perturbs the interaction between Tag and other subunits of pol-prim (27, 29, 30), we compared the ability of K425E and WT Tag to interact physically with primase and the N-terminal region of p180. Purified heterodimeric human primase or His-tagged p180 1–323 was incubated with anti-Tag antibody beads alone or in the presence of increasing amounts of WT or mutant Tag. After the beads were washed, bound proteins were detected by denaturing gel electrophoresis and immunoblotting. The amounts of primase bound to WT and K425E Tag were very similar (Fig. 3*B*, compare *lanes 2* and *3* with *lanes 4* and *5*). Moreover, the amounts of p180 1–323 bound to WT and K425E Tag were very similar (Fig. 3*C*, compare *lanes 2* and *3* with *lanes 4* and *5*). Taken together, the results support the interpretation that p68 binding to Tag is specifically reduced by the K425E charge reversal.

To verify this finding in the context of the intact pol-prim complex, increasing amounts of purified pol-prim were incubated with anti-Tag beads in the absence or presence of WT or K425E Tag. Bound pol-prim was detected by immunoblotting with anti-p180 antibody (Fig. 3*D*). No detectable pol-prim was bound to the beads in the absence of Tag (*lane 1*). K425E Tag (*lanes 4* and *5*) bound nearly as much pol-prim as did WT Tag (*lanes 2* and *3*), consistent with loss of only the low affinity p68-Tag docking (36) and retention of the contacts with primase and p180. Taken together, the results suggest that the K425E substitution specifically abrogates p68 docking without gross perturbation of Tag binding to other pol-prim subunits.

Because mutations in the p68N domain of pol-prim that weakened or prevented its physical interaction with Tag diminished or abolished SV40 primosome activity on RPA-coated ssDNA (36), we expected that primosome activity of K425E Tag should also be compromised. To assay primosome activity of K425E Tag independently of origin DNA unwinding, we utilized natural ssDNA saturated with RPA as the template. RPA inhibits the ability of pol-prim to generate RNA primers on the template and extend them into RNA-DNA products (32–34). RNA primer synthesis can be monitored directly by polymerization of radiolabeled ribonucleotides. However, extension of unlabeled RNA primers into dCTP-radiolabeled RNA-DNA primers amplifies the signal significantly and was therefore adopted as a more sensitive measure of primosome activity (22, 36, 41).

As expected, the ability of pol-prim to synthesize primers on naked ssDNA and extend them into radiolabeled RNA-DNA products was substantially inhibited when the template was precoated with RPA (Fig. 3*E*, compare *lanes 7* and *8*). Also as expected, the addition of WT Tag to the reaction relieved the inhibition of pol-prim, stimulating the production of radiolabeled RNA-DNA in a concentration-dependent manner (Fig. 3*E*, *lanes 1–3*). In contrast, K425E Tag failed to relieve the RPA inhibition (Fig. 3*E*, *lanes 4–6*). Quantification of the products confirmed that the primosome activity of K425E Tag was reduced to essentially background level (Fig. 3*F*, compare *lanes 4–6* with *lane 7*). These results are consistent with the inter-

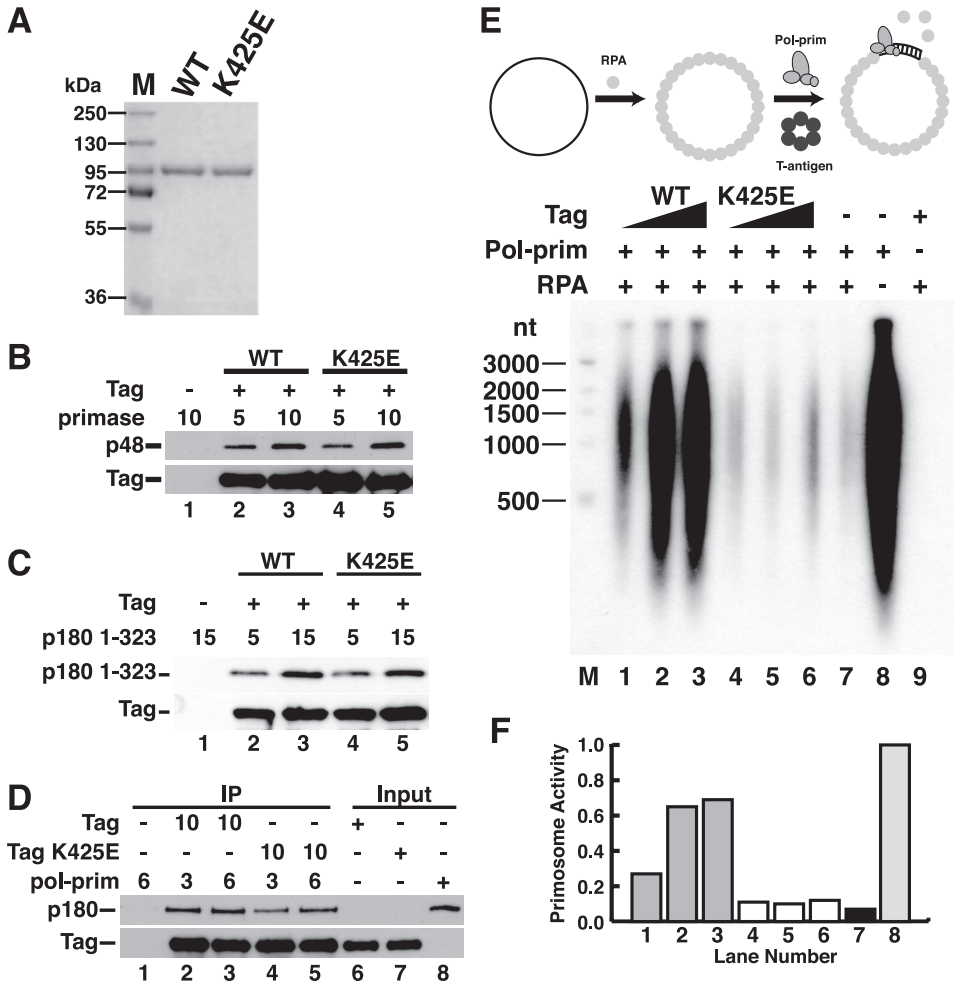

FIGURE 3. **K425E Tag binds to primase and p180 pol-prim but lacks primosome activity.** *A*, purified WT and K425E Tag were separated by SDS-PAGE and stained with Coomassie Brilliant Blue. *M*, protein size markers. *B* and *C*, Pab101 beads alone (*lane 1*) or bound to WT (*lanes 2* and *3*) or K425E Tag (*lanes 4* and *5*) were incubated with increasing amounts of primase dimer (*B*) or His-p180 1–323 (*C*) as indicated. Bound proteins were detected by SDS-PAGE and immunoblotting with anti-p48, anti-His (catalog no. A00186, Genscript), or Pab101 against Tag. *D*, anti-Tag beads alone (*lane 1*) or adsorbed to 10 μg of WT (*lanes 2* and *3*) or K425E Tag (*lanes 4* and *5*) were incubated with 3 or 6 μg of pol-prim as indicated. Bound proteins were analyzed by Western blotting with anti-Tag and anti-p180 antibody as indicated. *Input*, 100 ng. *E* and *F*, primosome activity of 200, 400, or 600 ng of Tag WT (*lanes 1–3*) or K425E (*lanes 4–6*) was assayed on 100 ng of ssDNA precoated with 1 μg of RPA in the presence of 600 ng of pol-prim. Control reactions lacked Tag (*lane 7*), Tag and RPA (*lane 8*), or pol-prim (*lane 9*). Reaction products were analyzed by alkaline electrophoresis and visualized by autoradiography (*E*). DNA size markers are shown (*M*). *F*, reaction products were quantified; signal in the negative control reaction (*lane 9*) was subtracted from that in *lanes 1–8*. Incorporation in *lanes 1–7* is expressed as a fraction of that in *lane 8*.

pretation that physical interaction of Tag with p68 is vital for primosome activity on RPA/ssDNA.

The K425E Substitution Inhibits Tag Helicase Activity and Origin DNA Unwinding-dependent Initiation of SV40 Replication—To determine whether the K425E substitution might also affect enzymatic functions of the Tag helicase domain, the ATPase activity of K425E Tag was assayed by monitoring radiolabeled inorganic phosphate released from labeled ATP (Fig. 4*A*). Indeed, the ATPase activity of K425E Tag was strongly reduced compared with that of WT Tag (compare *lanes 5–7* with *lanes 2–4*). Additionally, K425E Tag helicase activity was markedly lower than that of WT Tag (Fig. 4*B*, compare *lanes 8–10* with *lanes 4–6*).

Because the ATPase/helicase activity of Tag is required to unwind SV40 origin DNA to generate the template, K425E Tag would be expected to display a defect in origin-dependent initiation of replication. This prediction was tested in a monopolymerase reaction (41) using supercoiled DNA containing the SV40 origin and four purified proteins (T antigen, RPA, pol-prim, and topoisomerase I) with unlabeled ribo- and deoxyribonucleoside triphosphates and labeled dCTP. In the presence of WT Tag, radiolabeled RNA-DNA products accumulated in proportion to the amount of pol-prim present in the reaction (Fig. 4*C*, *lanes 1–3*), as expected, and no products were generated in the absence of Tag or pol-prim (*lanes 7* and *8*). Conversely, radiolabeled replication products were barely detectable in reactions containing K425E Tag, regardless of the amount of pol-prim present (*lanes 4–6*). These observations confirm that origin unwinding dependent-replication activity of K425E Tag is defective.

Is Tag ATPase/Helicase Activity Needed for Primosome Activity Independently of Origin DNA Unwinding?—The results from the monopolymerase assay (Fig. 4*C*) cannot distinguish whether the defective ATPase and helicase activities of K425E Tag (Fig. 4, *A* and *B*), its poor binding to p68 and defective primosome activity (Figs. 2 and 3), or a combination of these defects is responsible for the initiation defect. Therefore, it remains conceivable that ATPase/helicase activity of Tag contributes to primosome activity even when RPA/ssDNA is used as the template to bypass the requirement for origin DNA unwinding, as in Fig. 3. In that case, the ATPase defect of K425E Tag, rather than its defect in p68 docking, could be responsible for the loss of primosome activity observed in Fig. 3.

In order to evaluate the possibility that the ATP hydrolysis activity of Tag might play a vital role in primosome activity independently of origin DNA unwinding, we sought to inactivate Tag ATPase activity without affecting its interaction with pol-prim. Toward this end, we generated recombinant Tag with a substitution in the Walker B motif. The purified mutant protein D474N was stable and obtained in wild type yield (Fig. 5*A*). As expected, the D474N protein displayed very little ATPase activity (Fig. 5*B*, compare *lanes 2* and *3*) and no helicase activity (Fig. 5*C*). Also as expected, D474N Tag displayed little activity in an origin unwinding-dependent SV40 initiation assay (Fig. 5*D*, compare *lanes 1–3* with *lanes 4–6*).

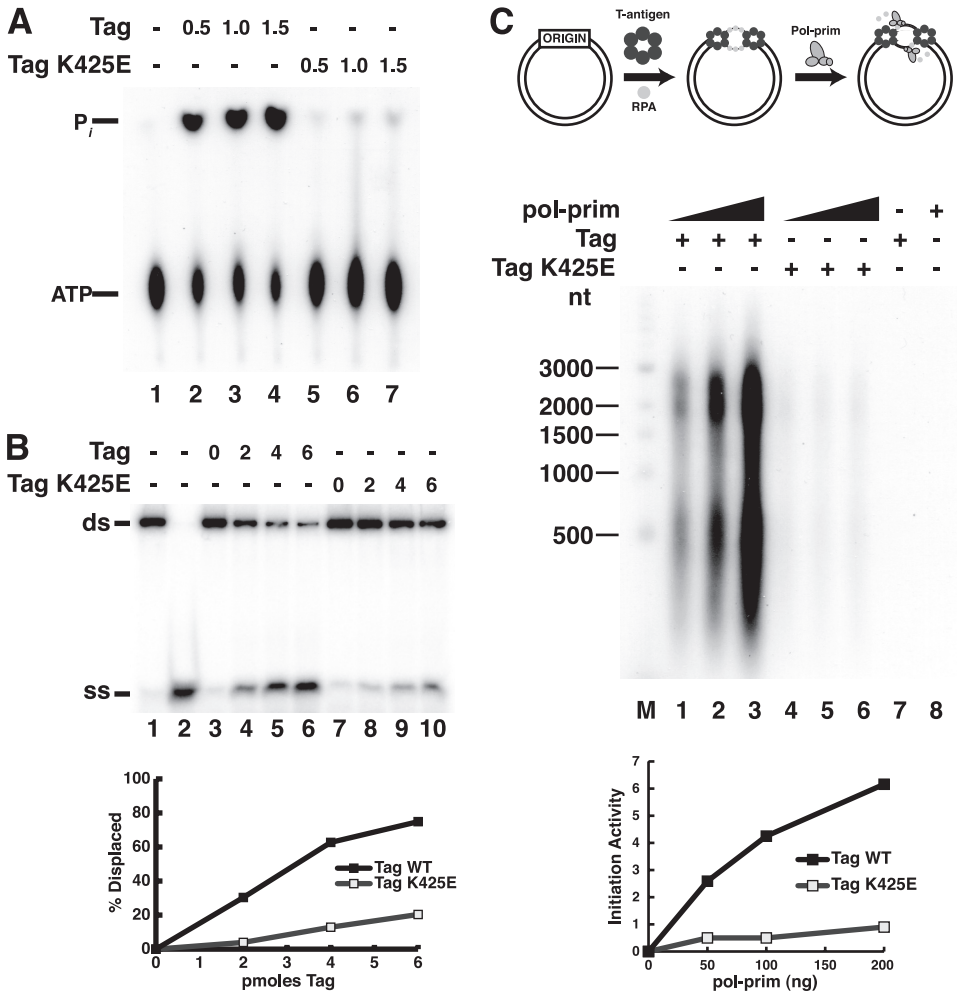

FIGURE 4. **K425E Tag is defective in ATPase activity and initiation of SV40 replication.** *A*, ATPase reactions were carried out without Tag (*lane 1*) or with increasing amounts of Tag WT (*lanes 2–4*) or K425E (*lanes 5–7*) as indicated. After 10 min, the reaction products were separated by ascending thin layer chromatography and visualized by autoradiography. *B*, to assess helicase activity, 10 fmol of DNA substrate was incubated without Tag (*lanes 3* and *7*) or with increasing amounts (2, 4, or 6 pmol) of WT (*lanes 4–6*) or K425E (*lanes 8–10*) Tag. *Lanes 1* and *2* contain DNA substrate or boiled substrate alone. *C*, SV40 initiation activity of Tag WT (*lanes 1–3*) or K425E (*lanes 4–6*) (600 ng) was assayed in monopolymerase reactions with 50, 100, or 200 ng of pol-prim. Radiolabeled DNA products were visualized by alkaline agarose electrophoresis and autoradiography. Products from control reactions without pol-prim (*lane 7*) or Tag (*lane 8*) are shown as indicated (−). End-labeled DNA fragments of the indicated sizes are shown at the *left* (*M*). Reaction products were quantified; background (*lanes 7 and 8*) was subtracted from incorporation in *lanes 1–6* (*lower panel*). *ss*, single strand; *ds*, double strand.

To detect possible changes in the interaction of D474N with pol-prim subunits, binding of p180 1–323, primase, and p68 to anti-Tag beads in the presence and absence of Tag was tested in pull-down assays. Both p180 1–323 (Fig. 6*A*) and primase (Fig. 6*B*) bound to the antibody beads in a Tag-dependent manner, with no significant difference between WT and D474N Tag (compare *lane 1* with *lanes 2* and *3* and with *lanes 4* and *5*). Last, p68 association with Tag D474N resembled that with WT Tag (Fig. 6*C*), indicating that ATPase/helicase activity is dispensable for physical interaction of Tag with the p68 subunit of pol-prim. Thus, Tag D474N appears to be a suitable protein to distinguish a potential role for Tag ATPase in primosome function independently of Tag docking with p68.

We then tested the activity of D474N Tag in the primosome assay. Importantly, D474N Tag relieved RPA-mediated inhibition of primer synthesis and extension on RPA/ssDNA template in a concentration-dependent manner, closely resembling the activity of the WT protein at equal concentrations (Fig. 6, *D* and *E*; compare *lanes 1–3* with *lanes 4–6*). This result demonstrates that Tag ATPase and helicase activity are dispensable for primosome activity on a preexisting RPA/ssDNA template.

DISCUSSION

A Specific p68N-docking Site on Tag Is Vital for SV40 Primosome Activity—We have mapped a p68-docking site on Tag that is disrupted by a charge reverse substitution K425E but not by a basic substitution K425R (Figs. 1 and 2). The positive charge of Lys^{425} is consistent with the expected electrostatic interaction with an acidic surface of p68N (36). Isothermal titration calorimetry of the binding interaction between the WT Tag and p68N indicated a low micromolar affinity typical of modular proteins, with both electrostatic and hydrophobic components (36, 46). The overall affinity of the pol-prim/Tag interaction (K_d = 12 nM) is more than 100-fold greater than that of Tag/p68 (K_d 6 μM), consistent with additional contacts between the Tag hexamer and other subunits of pol-prim (29, 30, 36). The K425E substitution in Tag does not appear to disrupt p180 or primase docking on Tag, suggesting that the substitution specifically weakens p68N binding (Figs. 2 and 3). Thus, p180 and primase probably contact distinct sites on the surface of the Tag hexamer, giving rise to the robust interaction with the four-subunit pol-prim.

A recent alanine-scanning analysis of Tag provided additional evidence for an important functional role for Lys^{425}. In a panel of 61 alanine substitutions in conserved, charged surface residues of the hexameric helicase domain, K425A was one of only six substitutions that, when individually tested in genomic SV40 DNA transfected into monkey cells, failed to generate viral progeny (45). Notably, alanine substitutions in each of the other three residues in the patch 4 mutant Tag did not reduce plaque formation. Moreover, the patch 4 mutant Tag retained the ability to transform rodent cells, in contrast with patch 1 and 2 mutant Tag variants that lost p53 or p300/CBP binding activity, respectively, as well as cell transformation activity (45).

Lys^{425} appears to be essential for Tag docking on p68N and SV40 primosome function (Figs. 2 and 3), confirming and extending the evidence for p68 docking on Tag in primosome

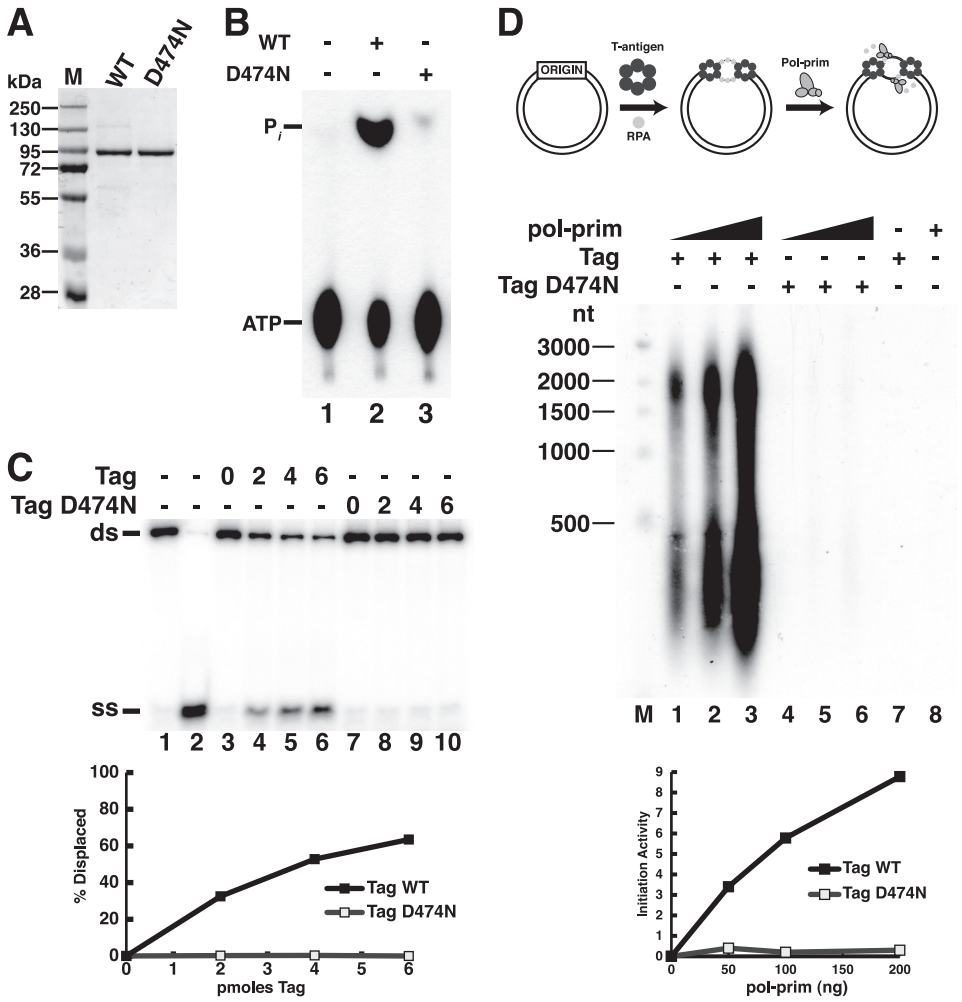

FIGURE 5. **A single residue substitution in the Walker B motif of Tag abolishes ATPase/helicase activity and initiation of SV40 replication.** *A*, purified WT and D474N Tag were separated by SDS-PAGE and stained with Coomassie Brilliant Blue. *M*, protein size markers. *B*, ATPase reactions were carried out without Tag (*lane 1*) or with 1 μg of Tag WT (*lane 2*) or D474N (*lane 3*). The reaction products were separated by ascending thin layer chromatography and visualized by autoradiography. *C*, to assess helicase activity, 10 fmol of DNA substrate was incubated without Tag (*lanes 3* and *7*) or with increasing amounts (2, 4, or 6 pmol) of WT (*lanes 4–6*) or D474N (*lanes 8–10*) Tag. *Lanes 1* and *2* contain DNA substrate or boiled substrate alone. *D*, SV40 initiation activity of 600 ng Tag WT (*lanes 1–3*) or D474N (*lanes 4–6*) was assayed in monopolymerase reactions with 50, 100, or 200 ng of pol-prim. Radiolabeled DNA products were visualized by alkaline agarose electrophoresis and autoradiography. Products of control reactions without pol-prim (*lane 7*) or Tag (*lane 8*) are shown as indicated (−). End-labeled DNA fragments of the indicated sizes are shown at the *left* (*M*). Reaction products were quantified; background (*lanes 7 and 8*) was subtracted from incorporation in *lanes 1–6* (*lower panel*). *ss*, single strand; *ds*, double strand.

function (36). Although an obvious potential role for p68-Tag docking in primosome function would be to recruit pol-prim, contacts of Tag with other pol-prim subunits are sufficient to maintain a strong interaction in the absence of p68N-Tag docking. Neither deletion of the N terminus of p68 (36) nor the Tag K425E charge reversal greatly diminished the interaction between Tag and pol-prim (Fig. 3, *B–D*). Thus, we postulate that p68-Tag docking, together with the interactions of p180 and primase with Tag, may be needed to properly position pol-prim in order to allow primase access to template DNA exposed by Tag-OBD contacts with RPA (36) (Fig. 1*A*). This would be consistent with the extreme species specificity of pol-prim in cell-free SV40 DNA replication. For example, although mouse and human pol-prim are highly conserved overall and Tag interacts physically with both enzymes, the spatial orientation of their Tag docking domains may differ, so that only primate pol-prim is active in the SV40 primosome (47–50). Moreover, although Lys^{425} is conserved among primate polyomavirus Tag proteins (45), it is not conserved among related viral helicases (*e.g.* papilloma virus E1 proteins), which also physically interact with and utilize pol-prim for viral DNA replication (51–53).

Architecture of the SV40 Primosome—The working model that pol-prim docking with the Tag helicase domain enables pol-prim to access the template exposed by local Tag-RPA remodeling implies that Tag may be a scaffold that positions the primosomal proteins for a molecular handoff reaction. Upon assembly with pol-prim, the relatively symmetric Tag hexamer would be transformed into an asymmetric primosome. In the primosome assay used here, the availability of RPA/ssDNA template bypasses the need for unwinding and allows stepwise dissection of the protein interactions required to assemble the primosome. The dispensability of Tag ATPase/helicase activity in this assay (Figs. 5 and 6), together with the requirement for Tag docking with RPA and pol-prim (Figs. 2 and 3) (22, 36), suggests that the interactions among these primosomal proteins may be sufficient to support primer synthesis and extension *in vitro*. Interestingly, the ATPase activity of the *E. coli* PriA fork restart helicase is also dispensable for PriA-catalyzed primosome assembly *in vitro* (54, 55).

The identification of Lys^{425} as the first pol-prim-docking site mapped on Tag provides some clues to the overall architecture of the viral primosome. Analysis of several hexameric helicases indicates that as the helicase tracks along one strand at the fork, either 5′–3′ in prokaryotes or 3′–5′ in archaea and eukaryotes, displacing the other strand, the motor domains face the duplex DNA (1, 4, 56–60). In prokaryotic primosomes, the primase docks on (or is fused to) the N-terminal domain of the helicase and thus follows behind as the helicase tracks on the lagging strand template. In contrast, the p68-docking site at Lys^{425} resides on the C-terminal face of the AAA+ domains in the Tag hexamer (Fig. 2*A*, *blue residues*), facing the duplex DNA as Tag tracks on the leading strand template (Fig. 7).

If pol-prim docks at the leading face of the Tag helicase, as our data suggest, how might the SV40 primosome initiate Oka-

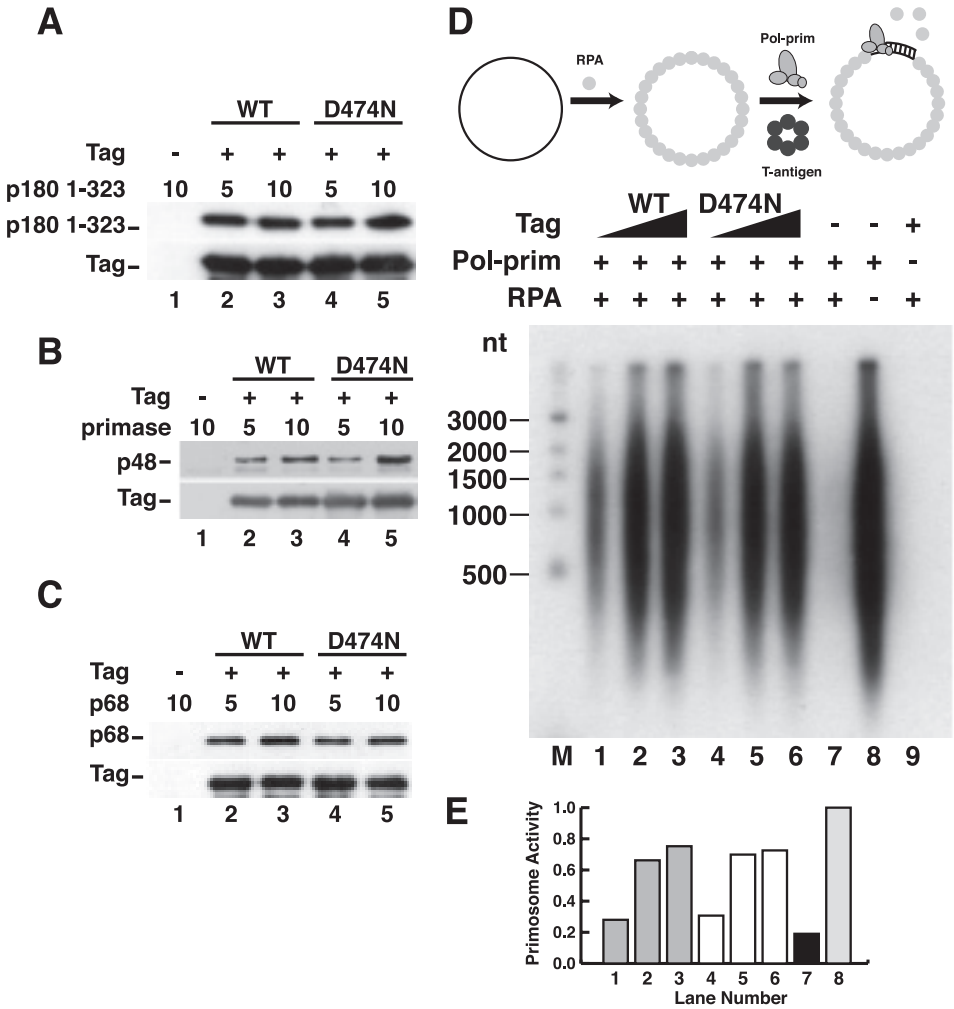

FIGURE 6. **ATPase activity of Tag is not required for pol-prim binding or primosome activity on RPA-coated ssDNA.** *A–C*, purified Tag WT or D474N bound to Pab101-coupled Sepharose beads was incubated with increasing amounts of His-p180 1–323 (*A*), primase dimer (*B*), or His-p68 (*C*) as indicated (in μg). Proteins bound to the beads were separated by SDS-PAGE and visualized by Western blotting with anti-His (catalog no. A00186, Genscript) for p180, anti-p48 or anti-His (catalog no. 9801, Abcam) for p68, and Pab101 against Tag. *D*, primosome activity of 200, 400, or 600 ng of Tag WT (*lanes 1–3*) or D474N (*lanes 4–6*) was assayed on 100 ng of ssDNA precoated with 1 μg of RPA in the presence of 600 ng of pol-prim. Control reactions lacking Tag (*lane 7*), Tag and RPA (*lane 8*), or pol-prim (*lane 9*) are indicated. Reaction products were analyzed by alkaline electrophoresis and autoradiography. DNA size markers are shown (*M*). *E*, reaction products were quantified; signal in the negative control reaction (*lane 9*) was subtracted from that in *lanes 1–8*. Incorporation in *lanes 1–7* is expressed as a fraction of that in *lane 8*.

zaki fragments on the lagging strand template? When the p68N domain docks at Lys^{425}, it is tethered through an apparently unstructured linker (residues ~80–205) to the C-terminal p68 domain (residues 206–598), which in turn is tightly complexed with the C-terminal zinc domain of the p180 subunit (36, 61) (Fig. 7). The p58 subunit of the primase heterodimer is also complexed with the p180 zinc domain (5, 62). Cryoelectron micrographs of a complex containing the structured C-terminal domains of yeast p68 (or B-subunit) and p180 suggest that the human p180/p68 complex may be comparable in size with the hexameric Tag helicase domain (14, 61). Based on these structures and the current Tag/p68-docking data, we speculate that the catalytic domains of p180 and primase may be positioned at some distance from the helicase surface where the p68 N terminus docks (36). This flexible spatial relationship between Tag and pol-prim might facilitate pol-prim access to the lagging strand template, as suggested by a hypothetical model depicted in Fig. 7. Clearly, the p180- and primase-docking sites on Tag remain to be determined. Competition of p53 with pol-prim for binding to Tag (47, 63, 64) suggests that one of these docking sites may overlap with the p53-binding surface at the outer edge of each AAA+/D3 domain (44). Because other aspects of the model may also be tested experimentally, we anticipate that it may prove useful in developing a better understanding of eukaryotic primosomes.

Coordination of DNA Unwinding and Primosome Functions at the Fork—In the replisome, the primosome handoff reaction is coupled with ATP hydrolysis and parental strand separation (2). In prokaryotes, several mechanisms that coordinate primosome activity with DNA unwinding and coordinate lagging with leading strand replisome movement have been elucidated (2, 65–69). However, it is not known whether or how such mechanisms might operate in eukaryotic replisomes.

SV40 primosome activity appears to require interactions of a pol-prim heterotetramer with a Tag hexamer (29, 31, 36, 41, 70). These interactions are stabilized in the presence of ATP or a nonhydrolyzable ATP analog (29). Here we present evidence that ATPase/helicase activity is dispensable for primosome activity when RPA/ssDNA template is supplied (Figs. 5 and 6). Thus, SV40 primosome activity can be mutationally and biochemically uncoupled from DNA unwinding *in vitro*, raising the question of whether such uncoupling may occur transiently in the viral replisome during primer synthesis.

Consistent with this possibility, pol-prim has been reported to substantially inhibit Tag helicase activity in the presence of RPA (70). The requirements for this inhibition were essentially identical to those for primosome activity except that primer synthesis was dispensable. These observations raise the possibility that pol-prim docking on Tag may reduce or inhibit its helicase activity, perhaps pausing 3′–5′ helicase progression on the leading strand template to promote primosome activity on the lagging strand (Fig. 7). Dissociation of one or more subunits of pol-prim from the helicase after primer synthesis, extension into an RNA-DNA primer, or the switch to polymerase δ might "release the

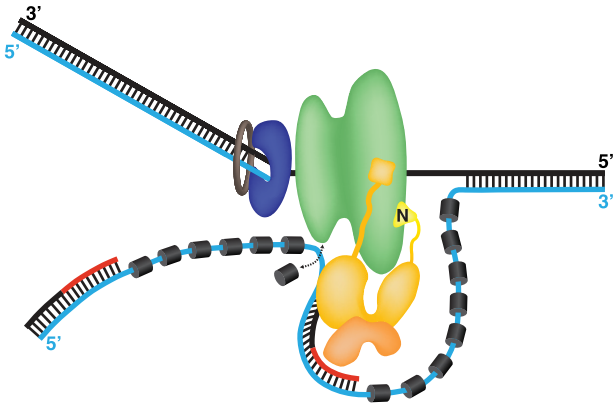

FIGURE 7. **Speculative model of the SV40 primosome at a replication fork.** A single Tag hexamer (*green*) tracking 3′–5′ on the leading strand template (*black*) is followed by DNA polymerase δ (*blue*)-proliferating cell nuclear antigen (*brown*) holoenzyme. The lagging strand template is displaced as Tag unwinds the duplex, but its point of exit from the helicase and its path after exit are controversial (17–20, 42, 43). Hence, the path depicted here is the simplest possibility. RPA (*dark gray cylinders*) bound to the lagging strand template (*cyan line*) is remodeled by specific contacts with the OBDs of the Tag hexamer into a weaker ssDNA-binding mode (22, 23, 35) that is easily displaced (*arrow*), exposing the template. The p180/p68 (*gold*) subunits of pol-prim contact the helicase domains of Tag through p68N (36) (see Figs. 1–3) and the N terminus of p180, which we propose are flexibly tethered to the pol-prim complex (27, 29, 30). The primase p58/p48 (*orange*) interaction surfaces with Tag are not known (30). Pol-prim correctly positioned on Tag is postulated to access the template exposed upon RPA remodeling, synthesize an RNA primer (*red line*), and extend it (*black line*), yielding an RNA-DNA primer. The subsequent proliferating cell nuclear antigen clamp loading and switch to DNA polymerase δ holoenzyme are not depicted (34, 71).

brakes" (34, 71). However, future work will be needed to elucidate how SV40 primosome activity is coordinated with DNA unwinding.

Acknowledgments—We thank J. M. Pipas, X. S. Chen, R. D. Ott, W. J. Chazin, B. E. Weiner, G. D. Guler, X. Zhao, B. Zhou, W. C. Copeland, W. P. Dulaney, G. Sowd, E. Kremmer, and H. Zhang for advice, reagents, cooperation, and discussion.

REFERENCES

1. Corn, J. E., and Berger, J. M. (2006) *Nucleic Acids Res.* **34,** 4082–4088
2. Hamdan, S. M., and Richardson, C. C. (2009) *Annu. Rev. Biochem.* **78,** 205–243
3. Langston, L. D., Indiani, C., and O'Donnell, M. (2009) *Cell Cycle* **8,** 2686–2691
4. Marians, K. J. (2008) *Nat. Struct. Mol. Biol.* **15,** 125–127
5. Copeland, W. C., and Wang, T. S. (1993) *J. Biol. Chem.* **268,** 11028–11040
6. Kuchta, R. D., and Stengel, G. (2010) *Biochim. Biophys. Acta* **1804,** 1180–1189
7. Kunkel, T. A., and Burgers, P. M. (2008) *Trends Cell Biol.* **18,** 521–527
8. Ilves, I., Petojevic, T., Pesavento, J. J., and Botchan, M. R. (2010) *Mol. Cell* **37,** 247–258
9. Gambus, A., van Deursen, F., Polychronopoulos, D., Foltman, M., Jones, R. C., Edmondson, R. D., Calzada, A., and Labib, K. (2009) *EMBO J.* **28,** 2992–3004
10. Aparicio, T., Guillou, E., Coloma, J., Montoya, G., and Méndez, J. (2009) *Nucleic Acids Res.* **37,** 2087–2095
11. Tanaka, T., and Nasmyth, K. (1998) *EMBO J.* **17,** 5182–5191
12. Walter, J., and Newport, J. (2000) *Mol. Cell* **5,** 617–627
13. Waga, S., and Stillman, B. (1994) *Nature* **369,** 207–212
14. Cuesta, I., Núñez-Ramírez, R., Scheres, S. H., Gai, D., Chen, X. S., Fanning, E., and Carazo, J. M. (2010) *J. Mol. Biol.* **397,** 1276–1286
15. Evrin, C., Clarke, P., Zech, J., Lurz, R., Sun, J., Uhle, S., Li, H., Stillman, B., and Speck, C. (2009) *Proc. Natl. Acad. Sci. U.S.A.* **106,** 20240–20245
16. Remus, D., Beuron, F., Tolun, G., Griffith, J. D., Morris, E. P., and Diffley, J. F. (2009) *Cell* **139,** 719–730
17. Wessel, R., Schweizer, J., and Stahl, H. (1992) *J. Virol.* **66,** 804–815
18. Smelkova, N. V., and Borowiec, J. A. (1997) *J. Virol.* **71,** 8766–8773
19. Reese, D. K., Meinke, G., Kumar, A., Moine, S., Chen, K., Sudmeier, J. L., Bachovchin, W., Bohm, A., and Bullock, P. A. (2006) *J. Virol.* **80,** 12248–12259
20. Meinke, G., Phelan, P., Moine, S., Bochkareva, E., Bochkarev, A., Bullock, P. A., and Bohm, A. (2007) *PLoS Biol.* **5,** e23
21. Weisshart, K., Taneja, P., and Fanning, E. (1998) *J. Virol.* **72,** 9771–9781
22. Arunkumar, A. I., Klimovich, V., Jiang, X., Ott, R. D., Mizoue, L., Fanning, E., and Chazin, W. J. (2005) *Nat. Struct. Mol. Biol.* **12,** 332–339
23. Jiang, X., Klimovich, V., Arunkumar, A. I., Hysinger, E. B., Wang, Y., Ott, R. D., Guler, G. D., Weiner, B., Chazin, W. J., and Fanning, E. (2006) *EMBO J.* **25,** 5516–5526
24. Bochkareva, E., Martynowski, D., Seitova, A., and Bochkarev, A. (2006) *EMBO J.* **25,** 5961–5969
25. Dornreiter, I., Höss, A., Arthur, A. K., and Fanning, E. (1990) *EMBO J.* **9,** 3329–3336
26. Dornreiter, I., Erdile, L. F., Gilbert, I. U., von Winkler, D., Kelly, T. J., and Fanning, E. (1992) *EMBO J.* **11,** 769–776
27. Dornreiter, I., Copeland, W. C., and Wang, T. S. (1993) *Mol. Cell Biol.* **13,** 809–820
28. Collins, K. L., Russo, A. A., Tseng, B. Y., and Kelly, T. J. (1993) *EMBO J.* **12,** 4555–4566
29. Huang, S. G., Weisshart, K., Gilbert, I., and Fanning, E. (1998) *Biochemistry* **37,** 15345–15352
30. Weisshart, K., Förster, H., Kremmer, E., Schlott, B., Grosse, F., and Nasheuer, H. P. (2000) *J. Biol. Chem.* **275,** 17328–17337
31. Ott, R. D., Rehfuess, C., Podust, V. N., Clark, J. E., and Fanning, E. (2002) *Mol. Cell Biol.* **22,** 5669–5678
32. Collins, K. L., and Kelly, T. J. (1991) *Mol. Cell Biol.* **11,** 2108–2115
33. Melendy, T., and Stillman, B. (1993) *J. Biol. Chem.* **268,** 3389–3395
34. Yuzhakov, A., Kelman, Z., Hurwitz, J., and O'Donnell, M. (1999) *EMBO J.* **18,** 6189–6199
35. Fanning, E., Klimovich, V., and Nager, A. R. (2006) *Nucleic Acids Res.* **34,** 4126–4137
36. Huang, H., Weiner, B. E., Zhang, H., Fuller, B. E., Gao, Y., Wile, B. M., Zhao, K., Arnett, D. R., Chazin, W. J., and Fanning, E. (2010) *J. Biol. Chem.* **285,** 17112–17122
37. Copeland, W. C. (1997) *Protein Expr. Purif.* **9,** 1–9
38. Weiner, B. E., Huang, H., Dattilo, B. M., Nilges, M. J., Fanning, E., and Chazin, W. J. (2007) *J. Biol. Chem.* **282,** 33444–33451
39. Henricksen, L. A., Umbricht, C. B., and Wold, M. S. (1994) *J. Biol. Chem.* **269,** 11121–11132
40. Gurney, E. G., Tamowski, S., and Deppert, W. (1986) *J. Virol.* **57,** 1168–1172
41. Matsumoto, T., Eki, T., and Hurwitz, J. (1990) *Proc. Natl. Acad. Sci. U.S.A.* **87,** 9712–9716
42. Li, D., Zhao, R., Lilyestrom, W., Gai, D., Zhang, R., DeCaprio, J. A., Fanning, E., Jochimiak, A., Szakonyi, G., and Chen, X. S. (2003) *Nature* **423,** 512–518
43. Gai, D., Zhao, R., Li, D., Finkielstein, C. V., and Chen, X. S. (2004) *Cell* **119,** 47–60
44. Lilyestrom, W., Klein, M. G., Zhang, R., Joachimiak, A., and Chen, X. S. (2006) *Genes Dev.* **20,** 2373–2382
45. Ahuja, D., Rathi, A. V., Greer, A. E., Chen, X. S., and Pipas, J. M. (2009) *J. Virol.* **83,** 8781–8788
46. Stauffer, M. E., and Chazin, W. J. (2004) *J. Biol. Chem.* **279,** 30915–30918
47. Murakami, Y., Eki, T., Yamada, M., Prives, C., and Hurwitz, J. (1986) *Proc. Natl. Acad. Sci. U.S.A.* **83,** 6347–6351
48. Schneider, C., Weisshart, K., Guarino, L. A., Dornreiter, I., and Fanning, E. (1994) *Mol. Cell Biol.* **14,** 3176–3185
49. Bullock, P. A. (1997) *Crit. Rev. Biochem. Mol. Biol.* **32,** 503–568
50. Simmons, D. T. (2000) *Adv. Virus Res.* **55,** 75–134
51. Park, P., Copeland, W., Yang, L., Wang, T., Botchan, M. R., and Mohr, I. J. (1994) *Proc. Natl. Acad. Sci. U.S.A.* **91,** 8700–8704
52. Masterson, P. J., Stanley, M. A., Lewis, A. P., and Romanos, M. A. (1998)

J. Virol. **72,** 7407–7419
53. Conger, K. L., Liu, J. S., Kuo, S. R., Chow, L. T., and Wang, T. S. (1999) *J. Biol. Chem.* **274,** 2696–2705
54. Zavitz, K. H., and Marians, K. J. (1992) *J. Biol. Chem.* **267,** 6933–6940
55. Gabbai, C. B., and Marians, K. J. (2010) *DNA Repair* **9,** 202–209
56. Bailey, S., Eliason, W. K., and Steitz, T. A. (2007) *Science* **318,** 459–463
57. Wang, G., Klein, M. G., Tokonzaba, E., Zhang, Y., Holden, L. G., and Chen, X. S. (2008) *Nat. Struct. Mol. Biol.* **15,** 94–100
58. Thomsen, N. D., and Berger, J. M. (2009) *Cell* **139,** 523–534
59. Pyle, A. M. (2009) *Cell* **139,** 458–459
60. McGeoch, A. T., Trakselis, M. A., Laskey, R. A., and Bell, S. D. (2005) *Nat. Struct. Mol. Biol.* **12,** 756–762
61. Klinge, S., Núñez-Ramírez, R., Llorca, O., and Pellegrini, L. (2009) *EMBO J.* **28,** 1978–1987
62. Mizuno, T., Yamagishi, K., Miyazawa, H., and Hanaoka, F. (1999) *Mol. Cell Biol.* **19,** 7886–7896
63. Braithwaite, A. W., Sturzbecher, H. W., Addison, C., Palmer, C., Rudge, K., and Jenkins, J. R. (1987) *Nature* **329,** 458–460
64. Gannon, J. V., and Lane, D. P. (1987) *Nature* **329,** 456–458
65. Lee, J. B., Hite, R. K., Hamdan, S. M., Xie, X. S., Richardson, C. C., and van Oijen, A. M. (2006) *Nature* **439,** 621–624
66. Pandey, M., Syed, S., Donmez, I., Patel, G., Ha, T., and Patel, S. S. (2009) *Nature* **462,** 940–943
67. Manosas, M., Spiering, M. M., Zhuang, Z., Benkovic, S. J., and Croquette, V. (2009) *Nat. Chem. Biol.* **5,** 904–912
68. Tanner, N. A., Hamdan, S. M., Jergic, S., Loscha, K. V., Schaeffer, P. M., Dixon, N. E., and van Oijen, A. M. (2008) *Nat. Struct. Mol. Biol.* **15,** 170–176
69. Hamdan, S. M., Loparo, J. J., Takahashi, M., Richardson, C. C., and van Oijen, A. M. (2009) *Nature* **457,** 336–339
70. Murakami, Y., and Hurwitz, J. (1993) *J. Biol. Chem.* **268,** 11008–11017
71. Waga, S., and Stillman, B. (1998) *Annu. Rev. Biochem.* **67,** 721–751
72. Kim, H. Y., Ahn, B. Y., and Cho, Y. (2001) *EMBO J.* **20,** 295–304
73. Luo, X., Sanford, D. G., Bullock, P. A., and Bachovchin, W. W. (1996) *Nat. Struct. Biol.* **3,** 1034–1039
74. Spence, S. L., and Pipas, J. M. (1994) *Virology* **204,** 200–209